Materials and Structures (2015) 48:471–484
DOI 10.1617/s11527-013-0197-z

ORIGINAL ARTICLE

Textile reinforced concrete (TRC) shells for strengthening and retrofitting of concrete elements: influence of admixtures

Michael Tsesarsky · Amnon Katz · Alva Peled · Oren Sadot

Received: 4 June 2013 / Accepted: 9 October 2013 / Published online: 15 October 2013

Abstract The mechanical behavior under impact loading of concrete elements strengthened with shells of textile reinforced concrete (TRC) was studied. The strengthening shells were made of either alkali-resistant glass or polyethylene (PE) fabrics that were impregnated with several cementitious matrices modified by common admixtures. Testing the strengthened elements for impact loading (strain rate from 0.4 to 1 s^{-1}) at flexure showed that the TRC reinforced elements conferred improved load capacity and impulse absorption. For glass strengthened TRC elements, the extent of the improvement depended on admixture grain size, such that smaller grain sizes were associated with better performance. For PE strengthened TRC elements, no similar dependency was found. These results correlate well with the behavior of the standalone TRC shells and with the properties of the fabrics themselves. PE TRC strengthened elements were found, via impulse loading tests, to have load carrying capacities comparable to those of elements strengthened with glass TRC, but without matrix additives. These findings suggest that low cost, commercially available PE textile could be used in TRC applications.

Keywords Textile reinforced concrete · Strengthening · Impact loading · Admixtures · Microstructure

M. Tsesarsky (✉) · A. Peled
Department of Structural Engineering, Ben-Gurion University of the Negev, POB 653, 84105 Beer-Sheva, Israel
e-mail: michatse@bgu.ac.il

M. Tsesarsky
Department of Geological and Environmental Sciences, Ben-Gurion University of the Negev, POB 653, 84105 Beer-Sheva, Israel

A. Katz
Faculty of Civil and Environmental Engineering, Technion-Israel Institute of Technology, 32000 Haifa, Israel

O. Sadot
Department of Mechanical Engineering, Ben-Gurion University of the Negev, POB 653, 84105 Beer-Sheva, Israel

1 Introduction

The combination of extreme events, natural or man-made, and dense human population centers emphasizes the need to develop sustainable and rigorous techniques for strengthening structural concrete elements. Indeed, the inherent brittleness and low tensile strength of most cement-based elements raise the concern that they may lack adequate strength, toughness and ductility to maintain their structural integrities under impact and other dynamic loads. Moreover, many structures worldwide antedate the establishment of modern building codes designed to mitigate the impact of dynamic loading. In the state of Israel, for example, about 100,000 concrete structures were built before the introduction in 1980 of design provisions that confer earthquake resistance on structures (SI 413). Thus, there is a need both for a method to structurally retrofit existing buildings that were built before institution of the relevant building codes and also for the creation of a design technique to be applied in newly constructed buildings to ensure they meet minimum load resistance requirements.

One of the most effective methods of enhancing the impact and blast resistance of concrete elements is to reinforce the concrete with fiber [1–7]. However, application of this solution to retrofit and strengthen existing concrete structural members is limited. High-modulus high-strength fabrics (e.g., carbon) impregnated with a polymeric matrix (typically epoxy) have also been shown to be effective in strengthening concrete structural elements and protecting them against failure under dynamic loads [8]. Despite their improved properties, however, the materials prepared using this technology have several limitations, including high cost, inability to withstand fire (unless expensive fire protection measures are applied), and incompatibility with the concrete substrate. Additional drawbacks include the relatively complicated application process, which involves careful preparation of the concrete substrate and the use of epoxy resin, the latter of which is hazardous to the health of the workers during the installation process.

A relatively new development in the preparation of such composite materials is textile-reinforced concrete (TRC), which comprises a combination of multi-axial fabrics and a fine-grained cementitious matrix. Such TRC composites have exhibited significantly improved tensile strength, ductility, and energy absorption properties compared with conventional, unadulterated concrete [9–11]. Moreover, orienting the main stress directions of the textiles so that they are parallel with the load direction provides a more effective solution than that obtained by randomly distributing short fibers in the concrete mix.

Several researchers have studied the applicability of textiles to the strengthening of concrete members subjected to loading [12–23]. Peled [21] investigated the potential of using cement impregnated textiles, compared to the conventional fabric-epoxy method, for the in situ strengthening and retrofitting of concrete columns. A Kevlar fabric–cement system used to repair concrete elements showed excellent compressive behavior. Even lower-modulus fabrics such as polypropylene exhibited some post-peak resistance, albeit to a lesser extent than was obtained with the Kevlar system. The flexural and shear strengthening of beams using cement-based textile composites and the bonding between the concrete and the composites were studied by Curbach and Ortlepp [14], who concluded that properly designed textiles combined with inorganic binders have good potential as strengthening materials for reinforced concrete members.

Indeed, recent works have shown that the impact and dynamic behaviors of TRC are markedly better than those of conventional cement reinforcement with short fibers [24–27]. Tsesarsky et al. [25] studied the extent to which carbon, glass and polyethylene (PE) fabrics fortify concrete elements when incorporated as part of the TRC layer. Although the carbon fabrics were reported to be the strongest, they also had the lowest reinforcing efficiency due to the poor penetrability of the cement between the filaments. The system with the PE fabric exhibited considerable post peak static and impact loading, resulting in high energy and impulse absorbance relative to glass.

In this research we studied the flexural properties of TRC shells, made using one of two commercially available fabrics, alkali resistant (AR) glass fabric and PE fabric, and of the concrete elements strengthened using these TRC shells. AR glass fabric is a commercial fabric with good adhesion to cementitious matrices that is widely used in the construction industry for mortar applications. PE fabric is a low-cost commercial fabric commonly used for shading in parks, outdoor sports facilities, and similar. The specific objective of the research was to study the effect of admixtures to the cementitious matrix of the TRC shell on load capacity and energy absorption of the strengthened concrete element when subjected to impact loading. The mechanical properties of stand-alone TRC shells and the TRC microstructure were examined vis-à-vis its impact behavior.

This work is part of the ongoing research in our laboratories to develop a technology for improving in situ the resistance of concrete structural elements to dynamic loading conditions by enclosing those elements in TRC layers that comprise a textile fabric impregnated with a cement-based material. The

Table 1 Properties of fabric and poltruded TRC shells

Fabric	ϕ (mm)	ρ (#/mm)	σ_{yr} (MPa)	E_{yr} (GPa)	t (mm)	V_f (%)
PE	0.5	0.37	240	1.8	9	3
Glass	0.3	0.28	1,372	72	8	1

ϕ is yarn diameter, ρ is yarn density, σ_{yr} is yarn tensile strength, E_{yr} is yarn modulus of elasticity, t is TRC shell cross-section thickness, and V_f is volume fraction of the fabric

Table 2 Properties of cement and admixtures used in the manufacture of TRC shells

Admixture	wt%	Particle size (μm)	Remarks
Plain cement (PC)	100	10	
Polymer (PL)	5	0.1	Film forming
Polypropylene chopped filaments (PPF)	0.1	12 (L = 10 mm)	
Fly ash (FA)	25	10	Pozzolanic
Silica fume (SF)	7	<1	Pozzolanic

concrete cores used in the study, therefore, were not reinforced with steel bars. This work constitutes an essential stage in the development and up-scaling of TRC technology toward its practical application in the reinforcement of concrete elements.

2 Experimental methods

2.1 Fabrics and matrices

Two fabrics with significantly different mechanical performances were used in the preparation of the TRC shells for this study: (i) AR glass in leno bonded fabric, made of coated bundles, and (ii) monofilament PE in a short weft-warp knitted fabric whose warp yarns, which were knitted into stitches, bound a set of yarns that were laid alternatingly in weft and warp directions. AR glass is a high-strength, high-modulus, multifilament yarn while the PE is a low-modulus, low-strength, monofilament yarn (Table 1). Note that the fabrics were tested to determine their mechanical properties and observed under SEM to measure their dimensions. Density in Table 1 was taken from the literature.

Different cementitious matrices were used to prepare the TRC shell composites. All matrices were based on CEM I 52.5N plain cement paste (PC) with a 0.4 water/cement ratio. Four different admixtures were used to investigate potential improvements to both fiber-matrix and TRC shell-concrete interaction: acrylic polymer (PL), polypropylene chopped fibers (PPF), fly ash type F (FA), and silica fume (SF). Admixtures particle sizes and fraction in cement paste are presented in Table 2.

2.2 TRC elements—sample preparation

To study the properties and behaviors of TRC as a standalone layer—not as part of the concrete element—laminated TRC shells were prepared from the different fabrics and matrices using the pultrusion technique. In this process the fabric passed through a slurry infiltration chamber where it was coated and thereafter it was pulled through a set of rollers both to force the paste between the fabric openings and to remove any excess paste [11]. Fabric–cement composites, laminated sheets measuring 250 mm × 300 mm and cast at varied thicknesses, were then formed on a plate-shaped mandrel. Cement boards were made with four layers of fabric similar to the TRC layers wrapped around the concrete elements (described below). The reinforcing yarns in the composites of each fabric were oriented in the pultrusion direction.

After the samples were produced, a constant load of about 50 N was applied to the fresh fabric–cement sheet surfaces to improve matrix penetration between the threads of yarn and openings in the fabric. The samples were then cured in water at room temperature for 28 days, after which they were cut into specimens measuring 25 mm × 150 mm (limited by the size of the available experimental set-up). The average thickness of the AR glass or PE composite was 8 or 9 mm, respectively, and the volume fraction of each was 1 or 3 %, respectively (Table 1). The TRC shells are described in more detail in Zhu et al. [27].

The wrapped concrete elements were prepared by first casting concrete plates that measured 400 mm × 400 mm × 40 mm and with a characteristic strength of 30 MPa. The plates were demolded 24 h after casting, after which they were cured for a total of 28 days: seven days in a water bath at room temperature, followed by 21 days in air at room temperature (RH = 50 %). Reference samples comprised plain concrete elements without TRC.

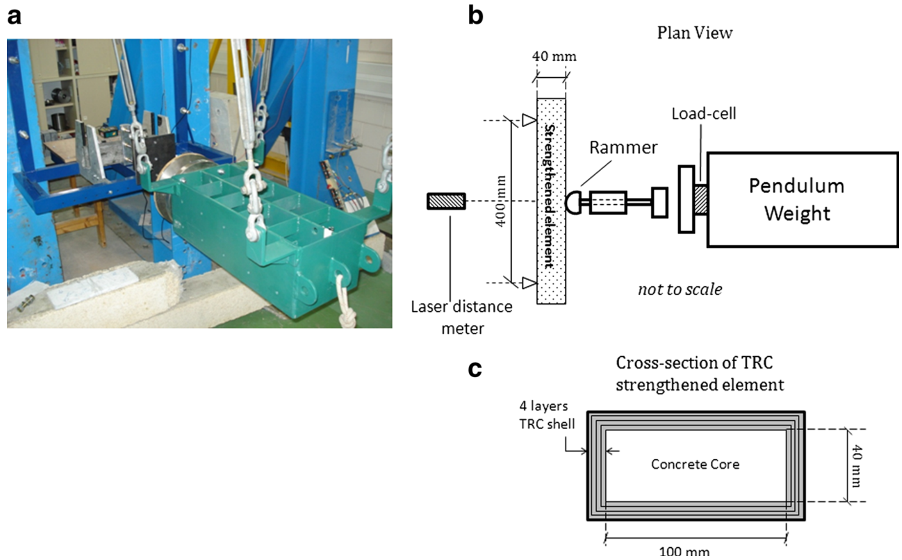

Fig. 1 Experimental setup of the impact flexural tests: **a** pendulum, **b** schematic plan view, and **c** cross-section of TRC strengthened element

At the conclusion of the 28-days curing process, the slabs were cut for impact tests into elements measuring 400 mm × 100 mm × 40 mm (limited by the size of the available experimental set-up). The surface of the concrete element was mechanically roughened until the underlying aggregate was exposed to facilitate better interaction between the concrete substrate and the TRC shell. To prepare the strengthened elements, the relevant fabric was immersed in one of the cement paste matrices with the different additives by the pultrusion technique as described above [10]. The impregnated fabric was then manually placed around the roughened surface of the cured concrete element, such that its reinforcing warp and weft yarns were parallel and perpendicular, respectively, to the long axis of the element. Four cement-impregnated fabric layers were used to produce an approximately 1-cm thick layer that was fully anchored to and that completely enveloped the concrete element (Fig. 1). The strengthened elements were cured in water at room temperature for additional 28 days and then in air (at ambient room conditions) until testing. Four strengthened elements of each admixture type (excluding SF) were tested in impact loading.

2.3 Static flexural loading

The standalone TRC shells (i.e., not applied to concrete elements) were tested under static flexural conditions on a MTS 810 loading frame with 100 kN load capacity. The shell was simply supported over a 110 mm span and centrally loaded at a rate of 0.5 mm min^{-1} (strain rate of $\sim$5 10^{-5} s^{-1}). Load and deflection of the beam were monitored continuously throughout the experiment, enabling the extraction of flexural stress and strain ($\varepsilon_f = 6\delta t/L^2$, where δ is the mid-span deflection, t is the thickness and L is the span between supports) and energy data (area under load–deflection curve).

2.4 Impact flexural loading

The concrete samples strengthened with TRC shells were tested under impact loading to assess their behavior under extreme conditions. The impact pendulum (Fig. 1a) is suspended by 5-m long cables. The weight of the basket alone is 62 kg, and additional 28 kg were added with lead blocks for a total of 90 kg. During the entire testing campaign drop height of the pendulum was set to 60 mm resulting in impact velocity of 1.1 m s^{-1}. The load was delivered to the sample via a rammer fitted with a linear bearing housing that enabled it to move freely and with little friction (Fig. 1b). The strain rate for the impact flexural tests ranged from 0.4 to 1.0 s^{-1}. The pendulum was equipped with a 55 kN load-cell (Honeywell type 47 10 V, 2 mV V^{-1}). The concrete elements enclosed within the TRC shells were tested using a three-point bending setup (Fig. 1b) with a clear span of 400 mm. Sample deflection was monitored using a Microtrack LTC 300 laser displacement meter (200 mm range with 10^{-3} mm accuracy). Data was

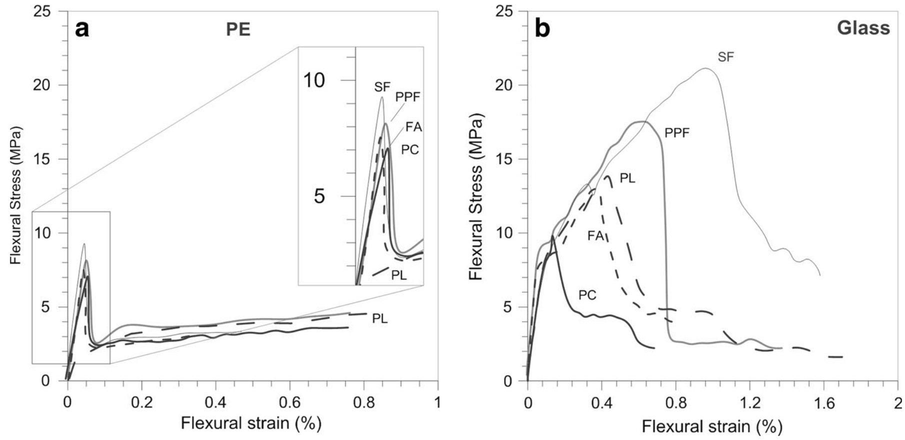

Fig. 2 Representative stress–strain curves for TRC shells in static flexural tests. *SF* silica fumes, *PL* polymer, *PPF* polypropylene fibers, *FA* fly ash and *PC* plain cement

acquired using a 1-Gs s^{-1} Oscilloscope (LeCroy WaveJet 314) with 8 bit vertical resolution (down to 2 mV div^{-1}) at a sampling rate of 100 or 200 kHz. The results were processed using a MatLab routine specifically developed for this project that included spectral analysis and re-sampling of the acquired signal to reduce noise.

2.5 Microstructure characteristics

TRC shell microstructures were characterized and correlated with shell mechanical properties. For these analyses, fragments of specimens obtained after flexural tests were dried at 60 °C and gold-coated. Microstructural features such as matrix penetration between the bundle and loop filaments of the fabrics were evaluated using a JOEL 840 scanning electron microscope (SEM).

3 Results

3.1 Static flexural loading—TRC shells

Representative stress–strain curves for static flexural loading of the TRC shells are presented in Fig. 2. PE fabric TRC shells (Fig. 2a), each with a different matrix containing either an FA, PPF or SF admixture, exhibited similar behaviors, such that the peak (ultimate) stress of each was in the range of 7–9 MPa at 0.05 % strain. Post-peak stress, which dropped to 2–3 MPa at 0.1 % strain for all three admixtures, was also very similar. Moreover, the drop in stress was followed by slight strain hardening and an increase to "steady state" values around 4 MPa. Behavior of the PC-PE TRC shell was similar, albeit with lower peak and residual values, while that of the PL-PE TRC shell differed post-peak, during which it exhibited constant strain hardening until a "steady state" value of 4–5 MPa was reached. These results indicate that the different admixtures had very little influence on the flexural properties of the TRC shells made with PE fabric.

Glass (g) TRC shell behavior (Fig. 2b) was strongly dependent on admixture type. The PC-g TRC attained a peak stress of 10 MPa at 0.12 % strain. At 0.35 % strain, the FA admixture improved flexural stress by about 30 % to 13 MPa, which increased to 14 MPa with the PL admixture at 0.4 % strain. Load capacity was considerably improved PPF, with a peak stress of 18 MPa at 0.65 % strain. The most prominent flexural stress improvement, peaking at 21 MPa at 0.9 % strain, was attained by the SF admixture. With the exception of the SF-g TRC, all glass TRC shell post peak behaviors were similar, exhibiting residual stress of about 2 MPa. These trends indicate that matrix type is a dominant factor for the glass TRC systems.

Figure 3 summarizes and compares the average peak stress and energy (the area under the load–deflection curve) values for both PE and glass TRC shells with the different matrix admixtures. The dashed horizontal line represents the flexural strength of an equivalent size cement paste shell (CEM I 52.5 using ASTM C78). For the PE TRC shells, with the exception of the PL TRC, for which the peak stress was lower by 32–48 % relative to other PE TRC shells tested, the different admixtures had only minor influences on load resistance. Likewise, energy

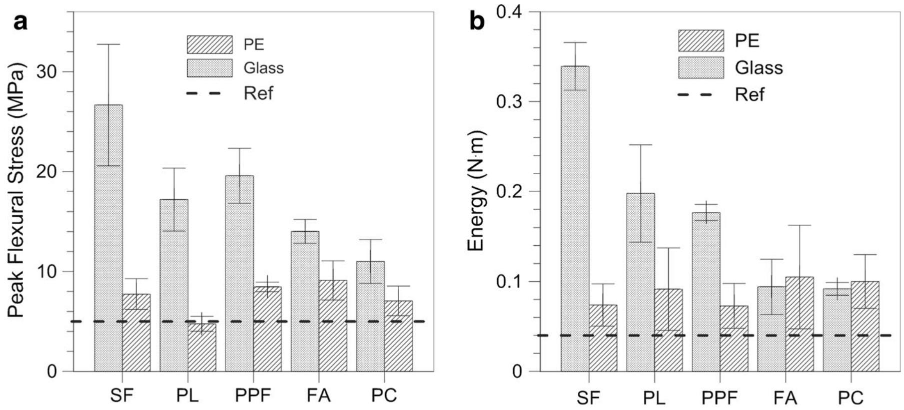

Fig. 3 Peak flexural stress **a** and energy **b** of TRC shells in static flexural tests. *SF* silica fumes, *PL* polymer, *PPF* polypropylene fibers, *FA* fly ash and *PC* plain cement. Energy for PE shells was computed for a deflection of 1.5 mm; for glass energy was computed for peak load. Reference values were computed for a concrete slab (typical strength 30 MPa) of dimensions similar to those of the TCR shells

absorption (Fig. 3b), which fell in the range of 0.073–0.1 Nm for all the TRC PE shells, was only negligibly dependent on admixture type. Energy absorption values were computed for deflections of 1.5 mm for SF, PPF, and FA. For PL, however, to account for its more ductile behavior, the PL admixture energy absorption value was computed for a deflection of 4 mm. Note that at 1.5 mm deflection the energy for PL was 50 % lower compared with the SF and PPF admixtures (0.037 vs. 0.074 Nm) and more than 60 % lower compared with FA and PC admixtures (0.037 vs. 0.1 Nm). These results again emphasize that, with the exception of PL, the tested admixtures had only small influences on the flexural behavior of the PE TRC shells. Compared with the plain paste reference sample without fabric (dashed line in the figure) the TRC PE shells exhibited energy values that were larger by two-fold than the reference value of 0.04 Nm. In addition, PE TRC shell stress values were also shown to improve relative to that of the reference, but to a lesser extent. These findings may indicate that, despite its low mechanical properties, PE fabric may confer some benefit as a strengthening material for concrete elements.

Glass TRC shells with SF, PL or PPF admixtures showed significantly improved load resistance compared to that of PC (Fig. 3a). Specifically, the SF admixture improved load resistance and energy absorption by 242 and 329 %, respectively, compared with those of the PC TRC. Similarly, the PL and PPF admixtures conferred on the glass TRC shell two-fold improvements in load resistance and energy absorption relative to the PC TRC. Both the stress and the energy results obtained for the FA admixture were similar to those observed for the PC.

A comparison of glass TRC and PE TRC shells clearly shows the former showed greater improvement than the latter as a result of incorporating matrix admixtures in TRC shell production. The strongest evidence for this finding is the greater than three-fold improvement, over PE TRC shells, in both load resistance and energy absorption for the glass TRC shells that included the SF admixture. Moreover, the use of the PL and PPF systems also elicited significant improvements in the load resistance and energy absorption of the glass relative to the PE TRC shells, which again suggests that the three tested admixtures highly benefit the TRC shell properties when glass fabrics were used. However, it is interesting to note that for the PC systems and those with the FA admixture, both PE and glass TRCs exhibited similar energy absorption (Fig. 3b), and although there is a significant difference in the mechanical properties of the two fabrics, use of the FA admixture conferred only a small advantage in strength on the glass TRC shell relative to the PE TRC shell (Fig. 3a). This is an important observation, especially in light of the low cost and good durability of the PE fabric relative to the glass.

3.2 Microstructural characteristics

To better understand the mechanisms controlling the different flexural behaviors of the TRC shells in terms

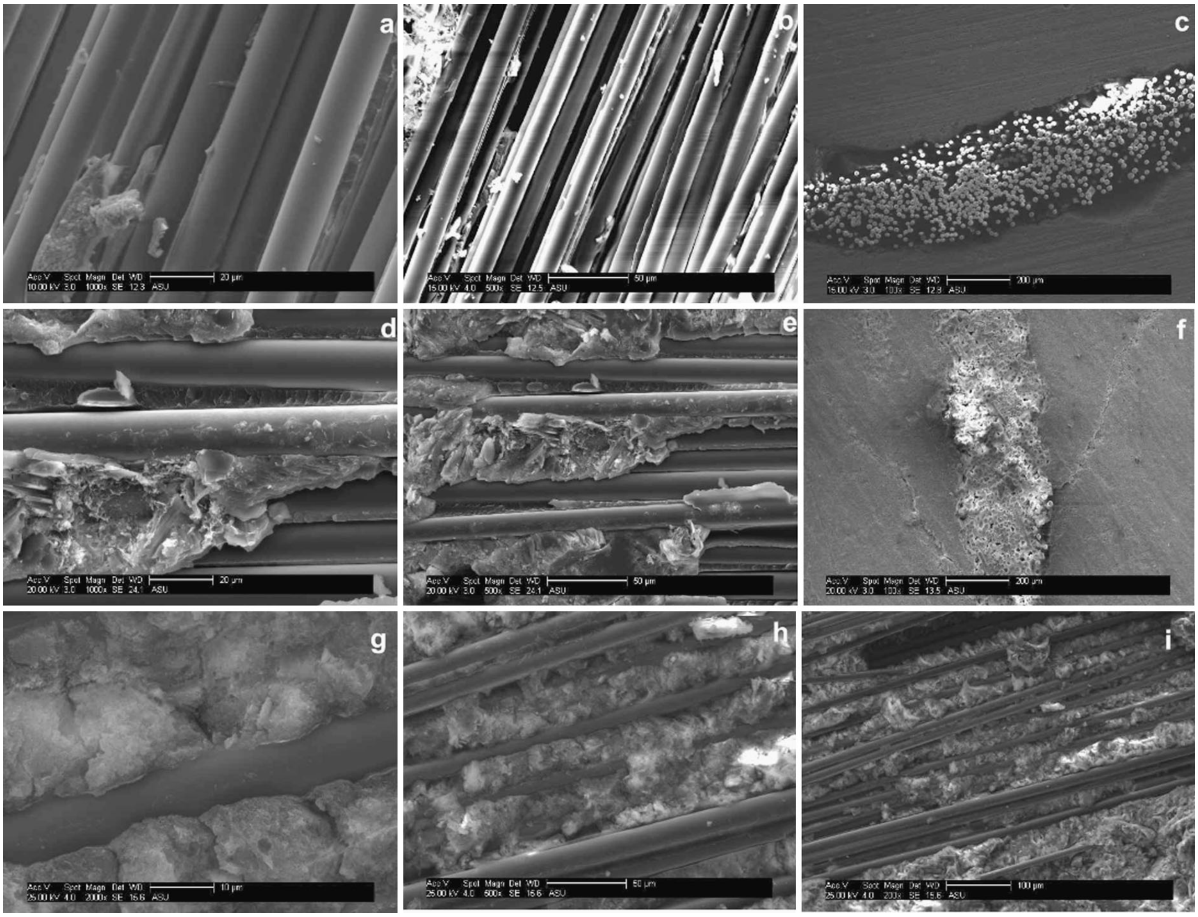

Fig. 4 SEM micrographs of Glass TRC shells. *Top panel*, PC matrix: **a** longitudinal view ×1,000 magnification, **b** longitudinal view ×500 magnification, **c** cross-sectional view ×100 magnification. *Middle panel*, SF matrix admixture: **d** longitudinal view ×1,000 magnification, **e** longitudinal view ×500 magnification, **f** cross-sectional view ×100 magnification. *Bottom panel*, PL matrix admixture: **g** longitudinal view ×2,000 magnification, **h** longitudinal view ×500 magnification, **i** longitudinal view ×200 magnification

of the admixtures and fabrics tested, TRC microstructures were observed and compared. Glass TRC shell (with PC, SF or PL matrix) microstructure is shown in Fig. 4. All images clearly show the multifilament structure of the glass yarn. The top panel (Fig. 4a–c) shows side views and a cross-sectional view of the glass multifilament yarn in the PC matrix; the middle panel (Fig. 4d–f) presents similar micrographs of the glass bundle in the SF matrix. The last panel (Fig. 4g–i) contains micrographs of the glass bundle in the PL matrix.

Poor cement matrix penetration between the filaments of the glass bundle is clearly observed in the cross-sectional micrograph of the PC matrix devoid of admixtures (Fig. 4c). Moreover, empty voids are evident between the matrix and the glass filaments along the bundle perimeter, an outcome indicative of poor bonding and inefficient stress transfer between matrix and filaments. The poor cement penetrability is also clear in the side views of the bundles with the PC matrix (Fig. 4a, b). At either magnification, hydration products are hardly seen between the filaments, which are interspersed instead with clearly visible empty spaces. Similar findings were also observed in the TRC glass shells with the FA admixture (not shown here), which also suffered from relatively poor matrix penetrability. In the case of the PC matrix, its inability to fill the spaces between the glass bundles may be attributed to the relatively large particle size of the cement, which impeded its penetration into the

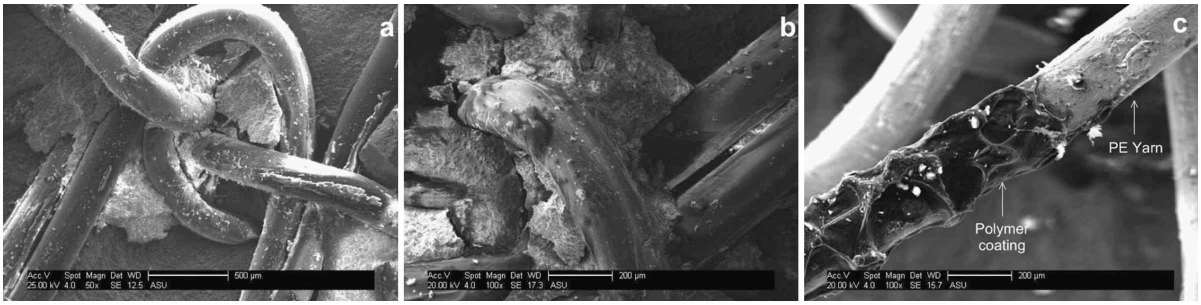

Fig. 5 SEM micrographs of PE TRC shell microstructure: **a** PE fabric loop in PC matrix, ×50 magnification, **b** PE fabric loop in PL matrix admixture, ×100 magnification, and **c** polymer coated PE yarn in PL matrix, ×100 magnification

interstitial spaces of the filament bundles, as described previously [9, 26, 28]. Particle size of the FA admixture particle size was similar to that of the cement, suggesting that their penetration behaviors will be similar.

In contrast to the inadequate penetration by the PC matrix, the SF admixture exhibited improved matrix impregnation of the glass bundles, as shown by the increase in hydration products clearly visible between filaments in both the longitudinal (Figs. 4d and e) and cross-sectional (Fig. 4f) micrographs. Moreover, the bundle perimeter shows almost no empty voids in the cross-section, which results in enhanced bonding (relative to bonding with the PC matrix) between the filaments and matrix and efficient stress transfer between the matrix and the entire bundle. The greater penetrability achieved by adding SF to the matrix may explain the improvement in load resistance, both peak values and energy, of the SF glass TRC relative to the PC glass TRC. Like SF, the PL admixture also promotes good penetrability by the cementitious matrix (Fig. 4g–i).

SEM micrographs of PE TRC shell microstructure (Fig. 5) clearly show the monofilament structure of the PE yarn. The loop's large diameter (~500 μm) facilitated matrix penetration in both cases presented (Fig. 5a, b) and partial anchoring of the loop in the matrix. Such an anchoring mechanism may explain the insensitivity of the mechanical properties to the type of matrix admixture, as discussed above.

Note that the surface of the PE yarn is covered in a polymeric layer in the PL matrix (Fig. 5c). The presence of this layer may result in low shear strength at the yarn-matrix interface and could be the main reason behind the lower load resistance, described previously, of the PE TRC. The addition of polymer to the cementitious matrix reduced, by 25 %, the load resistance in static flexure of the PE TRC shells relative to other admixtures used.

3.3 Impact flexural loading of TRC strengthened concrete elements

Representative load-time histories and impulse-time histories for the concrete elements strengthened with glass-PC and PE-PC TRCs are presented in Fig. 6. All systems were tested for impact using a 60-mm drop height of the pendulum (53 Nm input energy). Load-time curves clearly show that the TRC strengthened elements performed superiorly to the reference (REF) plain concrete system (Fig. 6a). Peak loads for the glass and PE-PC TRC systems were 9 and 6 kN, respectively, compared with only 3 kN for the reference element, thus showing that the TRC strengthened systems led to two- to threefold improvements.

The different systems tested also had significantly different loading durations: that of the reference was relatively short, ~0.003 s, compared to 0.012 s for the glass system (Fig. 6a). The load on the PE TRC strengthened element did not drop to zero but rather, it underwent protracted post peak loading (not shown to its final value to enable the display of all the systems in a single plot) until termination of the test. Impulse (the integral of load over time) revealed similar trends. Values for both glass and PE strengthened elements were higher by an order of magnitude than those of the reference system. It should be noted, however, that the ultimate impulse value for the PE system, due to its post-peak behavior, is higher than that presented in the figure to ensure that all the systems could be displayed in a single plot.

Post failure photos of representative glass and PE-PC TRC strengthened concrete elements are of either

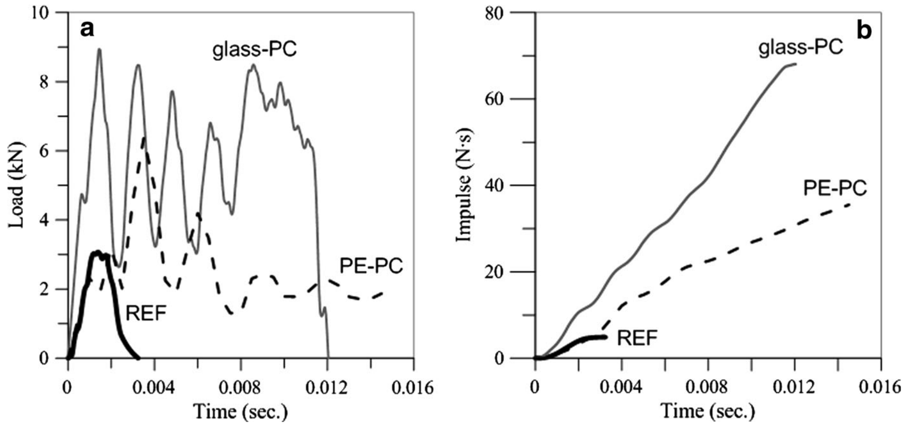

Fig. 6 Representative load-time (**a**) and impulse-time (**b**) curves for glass-PC and PE-PC TRC strengthened elements under full wrap application on roughened surfaces. The same data for a non-strengthened element are shown for reference

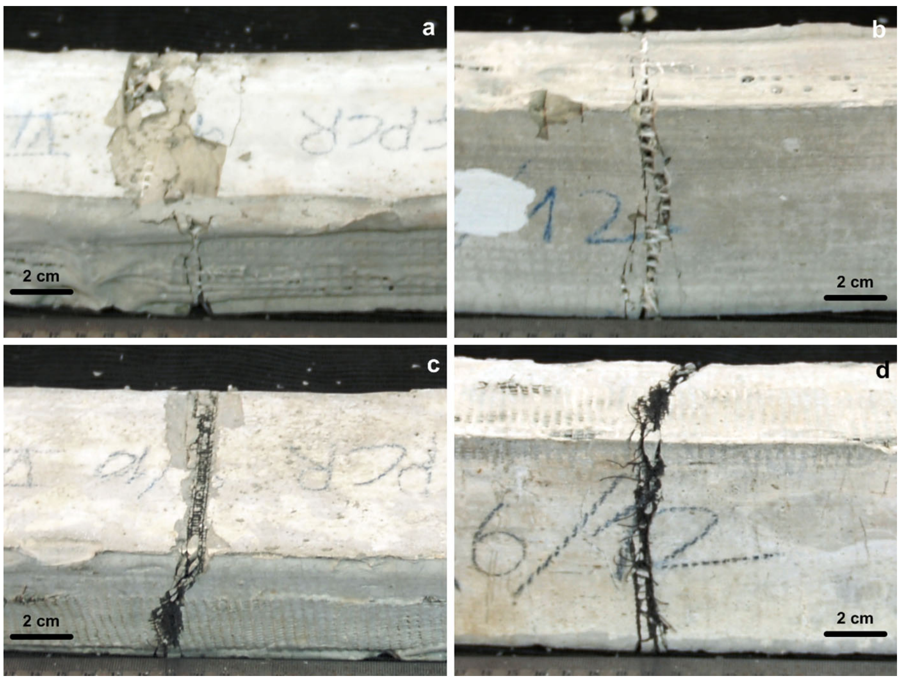

Fig. 7 Post failure images of glass (**a**, **b**) and PE TRC (**c**, **d**) strengthened elements. *Left* (**a**, **c**) are views of loaded face and *right* (**b**, **d**) are views of tensioned face

the compression (Fig. 7a, c) or the tension (Fig. 7b, d) faces of the elements. The failure mode for both glass and PE TRC strengthened elements was pull-out of the yarns out of the cementitious matrix. In either case, the sample did not fully rupture, instead exhibiting crack bridging in the tension zone with the development of a few cracks. The partial glass yarn pullout clearly visible in the tension zone is not observed for the PE yarns. In both cases the matrix in the compression zone suffered some damage that was more pronounced for the glass concrete element. Note that the concrete core, but not the TRC layer, was fractured, which shows the value of the TRC strengthening layer as a viable measure to prevent the fractured concrete element from disintegrating.

Figure 8 summarizes the average load capacity and average impulse absorbance of TRC strengthened concrete elements for PE and glass fabrics with the

Fig. 8 Load and impulse for PE and glass TRC strengthened elements under impact loading for full wrap application on a roughened surface. Additives to matrix include: *PL* polymer, *PPF* polypropylene fibers, *FA* fly ash and *PC* plain cement. PE impulse calculated to 0.1 s

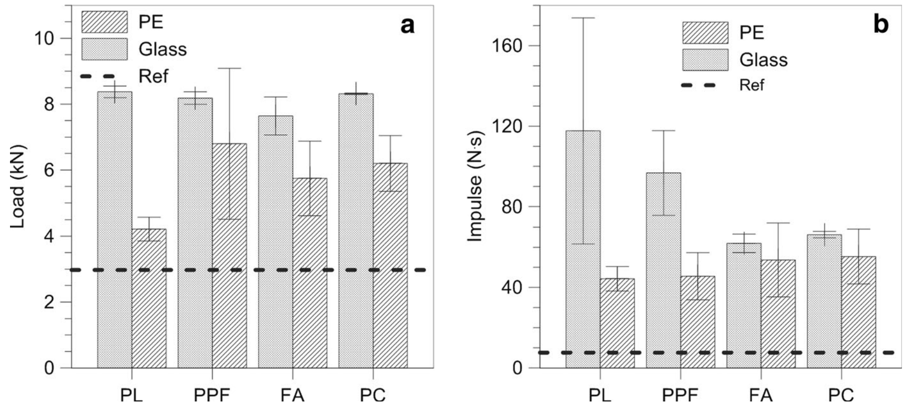

different matrix admixtures. The dashed horizontal line represents the load and impulse values for the reference concrete element (i.e., not strengthened with TRC). Similar peak loads of ~8 kN were observed for glass TRC strengthened concrete elements for all admixtures studied (Fig. 8a). PE TRC strengthened concrete elements also had similar, albeit lower, peak loads of ~6 kN for the PPF and FA admixtures and for PC. The peak load of the PE TRC strengthened concrete with the PL admixture, however, was considerably lower, ~4 kN. Thus, while only a modest improvement in load capacity of 33 % was achieved with the PE-PL TRC setup, in general, much larger improvements in peak load of 200–260 % were found for glass and PE TRC strengthening, respectively, compared to the reference element (~3 kN).

The impulse absorbance of glass TRC strengthened elements (Fig. 8b) was strongly dependent on matrix admixture: the PL and PPF admixtures had the maximum impulse absorbance values of 120 and 100 Ns, respectively, while those of the FA and PC admixtures were lower than those of the PL and PPF admixtures, the latter two of which were similar, ~70 Ns. Relative to the impulse absorbance of the reference element, those of the tested admixtures were up to an order of magnitude greater. Impulse absorbance of PE TRC strengthened elements was computed according to a loading duration of 0.1 s to account for the prominent post-failure deformation. The different matrix admixtures had similar impulse values ranging from 44 to 56 Ns. These values represent a four- to fivefold improvement in impulse absorbance relative to the reference element.

Also here, the concrete elements strengthened with glass TRC had higher load resistance (similar to the behavior of standalone TRC shells discussed above) than those strengthened with the PE TRC. However, the difference between the two fabric systems was smaller than that between the shells. The impulse absorption values of the glass TRC strengthened elements were also greater than those of the PE TRC strengthened elements, especially for the PL and PPF admixtures. The FA and PC admixtures had similar impulse values for both fabrics, despite the significant difference in mechanical properties of the two fabrics. This is again an important observation, mainly when considering fabric cost and durability.

During the course of the research, the testing at late age of several samples revealed that impulse absorption of the glass TRC strengthened elements deteriorated over time. This deterioration can be seen in the impulse ratios I_s/I_r, (where I_s and I_r are impulse of sample and reference element, respectively) of elements tested at younger ages, i.e., less than three months, which are typically higher than those of elements tested at older ages (Fig. 9). Indeed, the impulse ratio of the young samples was 11, which decreased over the course of a year more than threefold to a ratio of 3. Visual examination of the failed samples revealed that the glass bundles of the strengthening shell experienced full breakage with almost no pull-out.

The aging mechanisms of AR glass were not studied in depth in this research. In general aging effect of AR glass can be attributed to different degradation processes mainly: (1) alkali corrosion of the glass filaments embedded in the cementitious matrix [29, 30]; (2) stress fatigue [31, 32] and (3) changes in the bond between matrix and fibers [33]. Recent works were reported by Butler and co-workers [34–36].

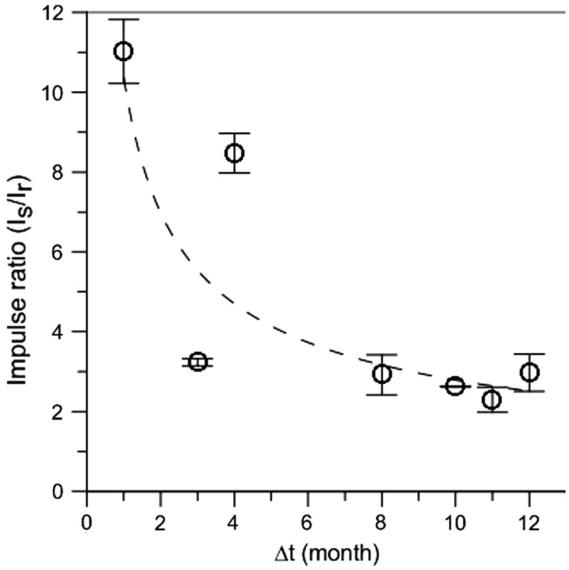

Fig. 9 Impulse ratio (I_s and I_r are impulse of sample and reference, respectively) as a function of time (Δt = time from end of curing to test) for glass TRC strengthened elements under full wrap application

It should be noted that PE TRC strengthened elements retained their impulse absorption properties over time and even showed some improvement, which was most likely due to later formation of hydration products as the TRC aged.

4 Discussion

Glass and PE TRC strengthened concrete elements exhibit different mechanical behaviors reflecting the properties and structures of each fabric and how those fabrics interact with the cementitious matrix. In general, correlation was found between the properties of the standalone TRC shells (i.e., not applied on the concrete) and, the properties of the TRC strengthened concrete elements tested under impact. The glass systems, both TRC shells and strengthened elements, exhibited better performance than the PE systems under static and impact conditions.

The high performance of the glass fabric, and its superior bonding with the cementitious matrix, can partly explain the superior qualities of the glass TRC. However, the similarity of PE and glass TRC shells with FA admixtures and PC matrices and of concrete elements strengthened with those shells does not adhere to this explanation. These results are consistent with those reported by Tsesarsky et al. [25], who showed, based on direct tension tests, that the reinforcing efficiency of a glass PC TRC shell (without matrix admixtures) was 33 % for a volume fraction of 1 % compared with 18 % efficiency for a volume fraction of 3 % for the PE TRC shell.

Another factor that affects the mechanical performance of the TRC shells and of the concrete strengthened with these shells is the interaction between fabric and matrix within the shell. In the case of the glass fabric (yarn), its multifilament structure and correspondingly high surface area can facilitate strong bonding when the matrix efficiently penetrates the spaces between the filaments. Cementitious matrix penetration of the bundles of glass yarns can facilitate more effective stress transfer from the external filaments to the inner filaments of the bundle. For the PE fabric (yarn), on the other hand, its monofilament structure and related small surface area result in lower interaction.

Matrix penetrability between the filaments of the glass bundle is strongly influenced by the addition of admixtures and, therefore, by the reinforcement efficiency of glass TRCs. The most significant improvement in flexure relative to that of the PC matrix was observed after the addition of silica fumes (SF), which facilitated better glass bundle penetration by the matrix. After SF, the polymer (PL) admixture was the next best performer, followed closely by the addition of chopped polypropylene fibers (PPF). A 0.1 % (by weight of cement) substitution by PPF was used to maintain cementitious matrix rheology. Despite this modest level of substitution, compared to the 2–5 % substitution for GFRC [1], the improvement was considerable. It is postulated that the addition of chopped fibers provides additional strength to the cementitious matrix by arresting localized cracking, thereby further improving the continuous strengthening of the fabric. The substitution of cement with 25 % (by weight) fly ash (FA) elicited only minor improvement. This finding can be explained by the weak penetration by the matrix of the glass bundle due to FA grain size, which is similar to that of the cement.

For the PE systems, both standalone TRC shells and strengthened elements, matrix admixtures, with the exception of PL, did not provide significant improvement under static or impact loading. In the case of the PE, the bonding was influenced mainly by mechanical anchoring of the loops within the matrix (Fig. 5). As

Table 3 Normalized peak strength and load ratios of TRC shells and TRC strengthened elements

Matrix	Static			Dynamic			Dynamic/static ratio
	Glass σ_p/σ_{ref}	PE σ_p/σ_{ref}	Glass/PE ratio	Glass L_p/L_{ref}	PE L_p/L_{ref}	Glass/PE ratio	
SF	5.33	1.55	3.44	N/A	N/A	N/A	N/A
PL	3.44	0.95	3.61	2.82	1.42	1.99	0.55
PPF	3.91	1.69	2.31	2.75	2.29	1.20	0.52
FA	2.80	1.82	1.54	2.57	1.93	1.33	0.86
PC	2.20	1.41	1.56	2.79	2.08	1.34	0.86

σ_p is the static peak flexural stress of TRC shells, $\sigma_{ref} = 5$ MPa, L_P is peak impact load, $L_{ref} = 3$ kN

the loop size of PE fabric is relatively large, all admixture types can penetrate the loops, yielding similar anchoring. The addition of PL to the cementitious matrix, however, reduced the load resistance in static flexure by 25 % relative to the other admixtures used. This can be partially explained by polymerization at the yarn-matrix interface (Fig. 5c), which may result in low shear strength at that interface. At this point, it is unclear why the addition of PPF did not improve the load resistance in a manner similar to that observed for the glass TRC shell.

Table 3 presents the normalized peak stresses for TRC shells in static flexure and normalized peak loads for TRC strengthened elements in impact loading. For each loading mode, the glass to PE ratio, which typically shows the advantage of the glass TRC relative to the PE TRC, is also presented. The dynamic to static ratio presents the efficiency loss of the TRCs in dynamic loading. Under static flexure, stress ratios range from 3.44 to 1.54, the values of which depend on the admixture matrix added to the glass TRCs. Under impact loading, this variation diminishes considerably, and the ratios range from 1.99 to 1.33. Finally, the dynamic to static ratio shows two distinct efficiency classes: first, the PL and PPF matrices with a ratio of $\sim$0.5, indicating that the glass TRC has a higher reinforcing efficiency relative to that of the PE TRC; and second, the PC and FA matrices with a ratio of 0.86, indicating that glass and PE TRCs possess similar reinforcing efficiencies.

The large-scale application of TRC strengthening based on high modulus and high price textiles (carbon, aramid, etc.) can quickly become impractical for non-critical structures, such as low-cost residential (public) housing, or in developing countries. The PE TRC strengthening shells provide considerable impulse absorption that, for PE TRC strengthened elements, is comparable with those of glass TRC strengthened elements for PC. The positive results of the PE fabric suggest therefore that it may serve as a low-cost alternative for strengthening concrete members with TRC shells. The use of a commercial, low-cost fabric and a cement based matrix without admixtures may facilitate an easy transfer of knowledge about this strengthening technique to developing countries with proven natural hazard. Further research on up-scaling of and cost-effectiveness PE TRC strengthened elements is required, before the technique is to be applied in situ.

4.1 Summary and conclusions

Two TRC strengthening systems based on AR glass and PE fabrics were studied. The fabrics were impregnated with cementitious matrices modified with an admixture comprising silica fumes (SF), polymer (PL), chopped polypropylene fibers (PPF) or fly ash (FA). In addition, a PC matrix was also studied. Standalone TRC shells not applied to concrete elements were studied under static flexure conditions. TRC strengthened concrete elements were studied for their flexural impact loading capacities.

The impact properties of the TRC strengthened elements were found to reflect the basic static loading properties of the TRC shells. Glass TRC shells showed consistent improvements in load capacity and energy absorption, depending on admixture type, from highest performance to lowest: SF, PL, PPF and FA and PC (tested as a reference). PE TRC shells showed similar load capacity and energy absorption, unrelated to admixture type.

The main factor controlling the mechanical behavior of the TRC shells investigated in this study was the basic fabric structure: multifilament leno bonded glass versus mono-filament warp knitted PE. The enhanced penetration by small diameter matrix admixtures, i.e., SF and PL, of the glass bundles facilitated enhanced bundle-matrix bonding and stress transfer compared with the lower penetration by large grain diameter admixtures such as FA and plain cement. Due to the monofilament structure of the PE yarn, this system is less sensitive to matrix grain size, and therefore, it exhibited similar mechanical behaviors for all the matrices under both static and impact loadings.

The low strength-high ductility PE TRC exhibited protracted post-peak load carrying capacity and energy absorption. Post-peak impulse values of PE TRC strengthened elements are similar to the impulse values exhibited by glass TRC strengthened elements with FA and PC matrices. These results are important, especially when considering the cost and durability of these fabrics.

The positive results of this study provide an impetus for further development of the PE fabric TRC technique for strengthening of concrete elements in regions of the world where dynamic (e.g., seismic) loading is probable and the use of high-end technical textiles is constrained by either cost or availability.

Acknowledgments Partial support by Israel Ministry for Construction and Housing is gratefully acknowledged.

References

1. Bentur A, Mindess S (2007) Fibre reinforced cementitious composites. Taylor and Francis, London
2. Besant T, Davies GAO, Hitchings D (2001) Finite element modelling of low velocity impact of composite sandwich panels. Compos A Appl Sci Manuf 32(9):1189–1196. doi:10.1016/s1359-835x(01)00084-7
3. Bharatkumar BH, Shah SP (2004) Impact resistance of hybrid fiber reinforced mortar. Paper presented at the international RILEM symposium on concrete science and engineering: a tribute to Arnon Bentur. Evanston
4. Bindiganavile V, Banthia N (2001) Polymer and steel fiber-reinforced cementitious composites under impact loading, part 2: flexural toughness. ACI Mater J 98(1):17–24
5. Suaris W, Shah SP (1983) Properties of concrete subjected to impact. J Struct Eng 109(7):1727–1741. doi:10.1061/(asce)0733-9445(1983)109:7(1727)
6. Xu H, Mindess S, IJ Duca (2004) Performance of plain and fiber reinforced concrete panels subjected to low velocity impact loading. In: M di Prisco, R Felicetti, Plizzari GA (eds) 6th RILEM conference on fiber reinforced Concret. BEFIB, Varenna pp 1257–1268
7. Zhang J, Maalej M, ST Quek, YY Teo Drop weight impact on hybrid-fiber ECC blast/shelter panels. In: Banthia N, Uomoto T, Bentur A, Shah SP (eds) Third international conference on construction materials: performance, innovation and structural applications. Vancouver, 2005
8. Teng JG, Chen JF, Smith ST, Lam L (2002) FRP strengthened RC structures, 1st edn. Wiley, Chichester
9. Brameshuber W (2006) Textile reinforced concrete—state-of-the-art report of RILEM TC 201-TRC
10. Peled A, Mobasher B (2005) Pultruded fabric–cement composites. Am Concr Inst Mater J 102(1):15–23
11. Peled A, Mobasher B (2007) Tensile behavior of fabric cement-based composites: pultruded and cast. J Mater Civ Eng 19(4):340–348. doi:10.1061/(asce)0899-1561(2007)19:4(340)
12. Brückner A, Ortlepp R, Curbach M (2008) Anchoring of shear strengthening for T-beams made of textile reinforced concrete (TRC). Mater Struct 41(2):407–418. doi:10.1617/s11527-007-9254-9
13. Contamine R, Larbi AS, Hamelin P (2013) Identifying the contributing mechanisms of textile reinforced concrete (TRC) in the case of shear repairing damaged and reinforced concrete beams. Eng Struct 46:447–458. doi:10.1016/j.engstruct.2012.07.024
14. Curbach M, Ortlepp R (2003) Besonderheiten des Verbundverhaltens von Verstaerkungsschichten aus textilbewehrtem. In: 2nd colloquium on textile reinforced structures. Dresden, pp 361–374 (in German)
15. Hegger J, Shams A, Kulas C, Horstmann M (2011) Application potential of textile reinforced concrete. In: Toledo RD, Silva FA, Koenders EAB, Fairbairn EMR (eds) 2nd international RILEM conference on strain hardening cementitious composites, vol 81. RILEM Proceedings pp 421–428
16. Larbi AS, Agbossou A, Hamelin P (2013) Experimental and numerical investigations about textile-reinforced concrete and hybrid solutions for repairing and/or strengthening reinforced concrete beams. Compos Struct 99:152–162. doi:10.1016/j.compstruct.2012.12.005
17. Larbi AS, Contamine R, Ferrier E, Hamelin P (2010) Shear strengthening of RC beams with textile reinforced concrete (TRC) plate. Constr Build Mater 24(10):1928–1936. doi:10.1016/j.conbuildmat.2010.04.008
18. Larbi AS, Contamine R, Hamelin P (2012) TRC and hybrid solutions for repairing and/or strengthening reinforced concrete beams. Eng Struct 45:12–20. doi:10.1016/j.engstruct.2012.06.002
19. Mechtcherine V (2013) Novel cement-based composites for the strengthening and repair of concrete structures. Constr Build Mater 41:365–373. doi:10.1016/j.conbuildmat.2012.11.117
20. Papanicolaou CG, Papantoniou IC (2010) Mechanical behavior of textile reinforced concrete (TRC)/concrete composite elements. J Adv Concr Technol 8(1):35–47
21. Peled A (2007) Confinement of damaged and nondamaged structural concrete with FRP and TRC sleeves. J Compos Constr 11(5):514–522. doi:10.1061/(asce)1090-0268(2007)11:5(514)
22. Weiland S, Hauptenbuchner B, Ortlepp R, Curbach M (2007) Textile reinforced concrete for flexural strengthening of RC-structures—part 2: application on a concrete shell. Paper presented at the design and applications of textile-reinforced concrete. Proceedings of the ACI Fall Convention, Puerto Rico

23. Wiberg A (2003) Strengthening of concrete beams using cementitious carbon fibre composites. Doctoral Thesis. Royal Institute of Technology, Stockholm
24. Haim E, Peled A (2011) Impact behavior of textile and hybrid cement-based composites. ACI Mater J 108(3):235–243
25. Tsesarsky M, Peled A, Katz A, Anteby I (2013) Strengthening concrete elements by confinement within textile reinforced concrete (TRC) shells—static and impact properties. Constr Build Mater 44:514–523
26. Zhu D, Gencoglu M, Mobasher B (2009) Low velocity flexural impact behavior of AR glass fabric reinforced cement composites. Cement Concr Compos 31(6):379–387. doi:10.1016/j.cemconcomp.2009.04.011
27. Zhu D, Peled A, Mobasher B (2011) Dynamic tensile testing of fabric–cement composites. Constr Build Mater 25(1):385–395. doi:10.1016/j.conbuildmat.2010.06.014
28. Cohen Z, Peled A, Pasder Y, Roye A, Gries T (2006) Effects of warp knitted fabrics made from multifilament in cement-based composites. In: Hegger J, Brameshuber W, Will N (eds) First international RILEM symposium on textile reinforced concrete. RILEM, Bagneux, pp 23–32
29. Larner LJ, Speakman K, Majumdar AJ (1976) Chemical interactions between glass fibres and cement. J Non Cryst Solids 20(1):43–74. doi:10.1016/0022-3093(76)90107-1
30. Majumdar AJ, West JM, Larner LJ (1977) Properties of glass fibres in cement environment. J Mater Sci 12(5): 927–936. doi:10.1007/BF00540975
31. Michalske TA, Freiman SW (1983) A molecular mechanism for stress corrosion in vitreous silica. J Am Ceram Soc 66(4):284–288. doi:10.1111/j.1151-2916.1983.tb15715.x
32. Orlowsky J, Raupach M (2008) Durability model for AR-glass fibres in textile reinforced concrete. Mater Struct 41(7):1225–1233. doi:10.1617/s11527-007-9321-2
33. Bentur A (2000) Role of interfaces in controlling durability of fiber-reinforced cements. J Mater Civ Eng 12(1):2–7. doi:10.1061/(ASCE)0899-1561(2000)12:1(2)
34. Butler M, Hempel S, Mechtcherine V (2011) Modelling of ageing effects on crack-bridging behaviour of AR-glass multifilament yarns embedded in cement-based matrix. Cem Concr Res 41(4):403–411. doi:10.1016/j.cemconres.2011.01.007
35. Butler M, Mechtcherine V, Hempel S (2009) Experimental investigations on the durability of fibre–matrix interfaces in textile-reinforced concrete. Cem Concr Compos 31(4): 221–231. doi:10.1016/j.cemconcomp.2009.02.005
36. Butler M, Mechtcherine V, Hempel S (2010) Durability of textile reinforced concrete made with AR glass fibre: effect of the matrix composition. Mater Struct 43(10):1351–1368. doi:10.1617/s11527-010-9586-8